Boreal forest cover was reduced in the mid-Holocene with warming and recurring wildfires

Martin P Girardin, Dorian M Gaboriau, Adam A Ali, Konrad Gajewski, Michelle D Briere, Yves Bergeron, Jordan Paillard, Justin Waito, Jacques C Tardif

communications earth & environment

Article

https://doi.org/10.1038/s43247-024-01340-8

Boreal forest cover was reduced in the mid-Holocene with warming and recurring wildfires

Martin P. Girardin[1,2,3] ✉, Dorian M. Gaboriau[3], Adam A. Ali[3,4], Konrad Gajewski[5], Michelle D. Briere[5], Yves Bergeron[2,3], Jordan Paillard[6], Justin Waito[7] & Jacques C. Tardif[2,7]

The hemi-boreal zone, marking North America's southern boreal forest boundary, has evolved post-glaciation, hosting diverse ecosystems including mixed forests with savannas, grasslands, and wetlands. While human, climate, and fire interactions shape vegetation dynamics therein, specific influences remain unclear. Here we unveil 12,000 years of hemi-boreal zone dynamics, exploring wildfire, vegetation, climate, and human population size interactions at such long time scales. Postglacial biomass burning exhibited episodes of persistent elevated activity, and a pivotal shift around 7000 years ago saw the boreal forest transition to an oak-pine barren ecosystem for about 2000 years before reverting. This mid-Holocene shift occurred during a period of more frequent burning and a sudden uptick in mean annual temperatures. Population size of Indigenous peoples mirrored wildfire fluctuations, decreasing with more frequent burning. Anticipated increases of fire activity with climate change are expected to echo transformations observed 7000 years ago, reducing boreal forest extent, and impacting land use.

The circumpolar boreal forest is one of the largest and most extensive biomes on Earth[1]. Within this vast expanse, the hemi-boreal zone occupies a critical ecological area in North America. This transitional zone marks the southern limit of closed boreal forest and is home to mixed forests with a high diversity of tree species and communities including savannas, grasslands, and wetlands[1–3]. Towards the interior of the North American continent, at the prairie-forest ecotone, woody and herbaceous vegetation intermingle at many different scales[4]. The hemi-boreal zone acts as a biodiversity hotspot, with many species adapted to the transitional nature of the ecosystem[5,6]. This transitional zone also plays a key role in maintaining ecological processes such as nutrient cycling, carbon storage and sequestration, and regulation of the hydrological cycle[6–9].

The hemi-boreal zone, and more particularly the areas surrounding the prairie-forest ecotone, faces considerable environmental pressures affecting the functioning of the ecosystems[10,11]. Among different drivers, wildfire is a notable cause of ecosystem changes[12,13]. The prairie-forest ecotone's transitional nature, mix of vegetation types, and susceptibility to human-caused fires, along with the increased frequency and severity of wildfires driven by climate change and human ignition, make it particularly vulnerable. The interspersal of forests and wetlands with grasslands, which are naturally more fire-prone[14,15], facilities the rapid spread of fires. Land degradation due to logging, oil and gas exploration, and other human activities is another pressure on the prairie-forest ecotone[16,17]. Agriculture development along the southern fringe of the boreal zone is a large contributor to deforestation, although land-use allocations such as forest management agreements and zoning for forest and agricultural land use limit the expansion of agriculture into forests[18]. Invasive species also pose a risk to plant community structure, as they can outcompete native species and alter ecosystem processes[19]. Habitat loss and forest fragmentation can diminish biodiversity, thereby impacting ecosystem functioning and the provision of ecological services[20].

The boreal/hemi-boreal climate-vegetation-fire nexus described above has been under continuous change since the end of the last glaciation approximately 10,000 years ago[21]. Climate shaped the development of the prairie-forest ecotone by altering species distribution, stand structure, and

[1]Natural Resources Canada, Canadian Forest Service, Laurentian Forestry Centre, Québec, QC, Canada. [2]Centre d'étude de la forêt, Université du Québec à (UQAM), Montréal, Montréal, QC, Canada. [3]Institut de recherche sur les forêts, Université du Québec en Abitibi-Témiscamingue, Rouyn-Noranda, QC, Canada. [4]ISEM, Univ Montpellier, CNRS, IRD, EPHE, Montpellier, France. [5]Laboratory for Paleoclimatology and Climatology, Department of Geography, Environment and Geomatics, University of Ottawa, Ottawa, ON, Canada. [6]Département de Géographie, Université de Montréal, Montréal, QC, Canada. [7]Centre for Forest Interdisciplinary Research (C-FIR), The University of Winnipeg, Department of Biology/Environmental Studies & Sciences, Winnipeg, MB, Canada.
✉e-mail: martin.girardin@nrcan-rncan.gc.ca

forest regeneration[22]. While temperature limitations are largely responsible for the northern limit of the boreal forest[23], the southern boundary between the boreal forest and prairies is typically maintained by low precipitation and associated high fire frequency that limits the establishment of tree species[24]. Owing to the high degree of temporal and spatial variations typical of wildfire regimes in such regions, many landscapes have shifted between mosaics of open- and closed-canopy forests over the past millennia[22,25–27]. For example, the prairie–forest ecotone in south-central Minnesota saw shifts from boreal forest 12,500–10,000 cal. yrs. BP, to oak savanna forest 10,000–9000 cal. yrs. BP, changing to prairie-like communities and deciduous forest taxa 8000–4250 cal. yrs. BP, and finally shifting to a *Quercus*-dominated woodland/savanna between 4250 and 3000 cal. yrs. BP[28].

Frequent intentional burning is employed in savannas and seminatural grasslands to deter the expansion of woody vegetation, to promote the growth of fresh herbaceous vegetation, and to safeguard the landscape against potential destructive fires by utilizing patch burning at the onset of the burning season[29]. Although there is today a notable impact of human activities on these ecosystems, the impacts of burning practices by Indigenous peoples on the landscape during the Holocene are less known[30,31]. An extensive literature has argued that Indigenous burning has profoundly influenced the structure and location of the prairie-forest ecotone in North America[32,33]. However, other literature and a recent analysis of paleoenvironmental and paleodemographic data across the Northern American prairie-forest ecotone challenged the notion that Indigenous societies substantially altered past ecosystems of the region[21]. Integrating archeological, paleoecological, and paleoclimate data to infer human, fire, and vegetation interactions in this region faces challenges due to incomplete records, temporal misalignments among data sources, scale mismatches with Indigenous settlements, and reliance on proxies with limitations, introducing uncertainties in interpreting past ecosystems[34–37].

In this study, we document centennial- to millennial-scale variability in wildfire, vegetation, climate, and human population size dynamics at the prairie-forest ecotone of the hemi-boreal zone in North America, in order to shed light on the complex interactions and feedback among these factors at such long time scales. Specifically, using macro-charcoal found in sediment samples from six lakes, we investigated changes in the frequency, size, and severity of fire occurrences over the last 12,000 years. Additionally, from pollen analysis we reconstructed the postglacial vegetation response to fire disturbances, including changes in species composition. Next, we examined the influence of past climate change on fire regimes and vegetation dynamics using paleoclimatic model simulation outputs. Finally, by integrating archeological records with historical climate, vegetation, and fire data, we analyzed relationships among post-glacial human population size, climate drivers, and ecosystem dynamics. Our study demonstrates that around 7000 cal. yrs. BP, the hemi-boreal zone shifted from closed-type boreal forests to an oak-pine barren ecosystem. This shift was synchronized with a reshaping of fire dynamics and human population fluctuations. Findings from this research will contribute to the broader scientific understanding of the interactions among fire, climate, vegetation, and land-use, while providing insights into the resilience and sustainability of boreal ecosystems in the face of modern warming and fire disturbances.

Results

Sedimentation onsets and rates

The study area, located in the Lake of the Woods Ecoregion along the border between the provinces of Manitoba and Ontario in Canada (Fig. 1), was examined by sampling sediments from six lakes. The cores were collected in water columns reaching 1.2 m to 8.3 m depths (Table 1). Sediment core lengths of the six sampled lakes averaged 614 cm, ranging from 247 cm for Lake M14 to 818 cm for Lake O16 (as indicated by the

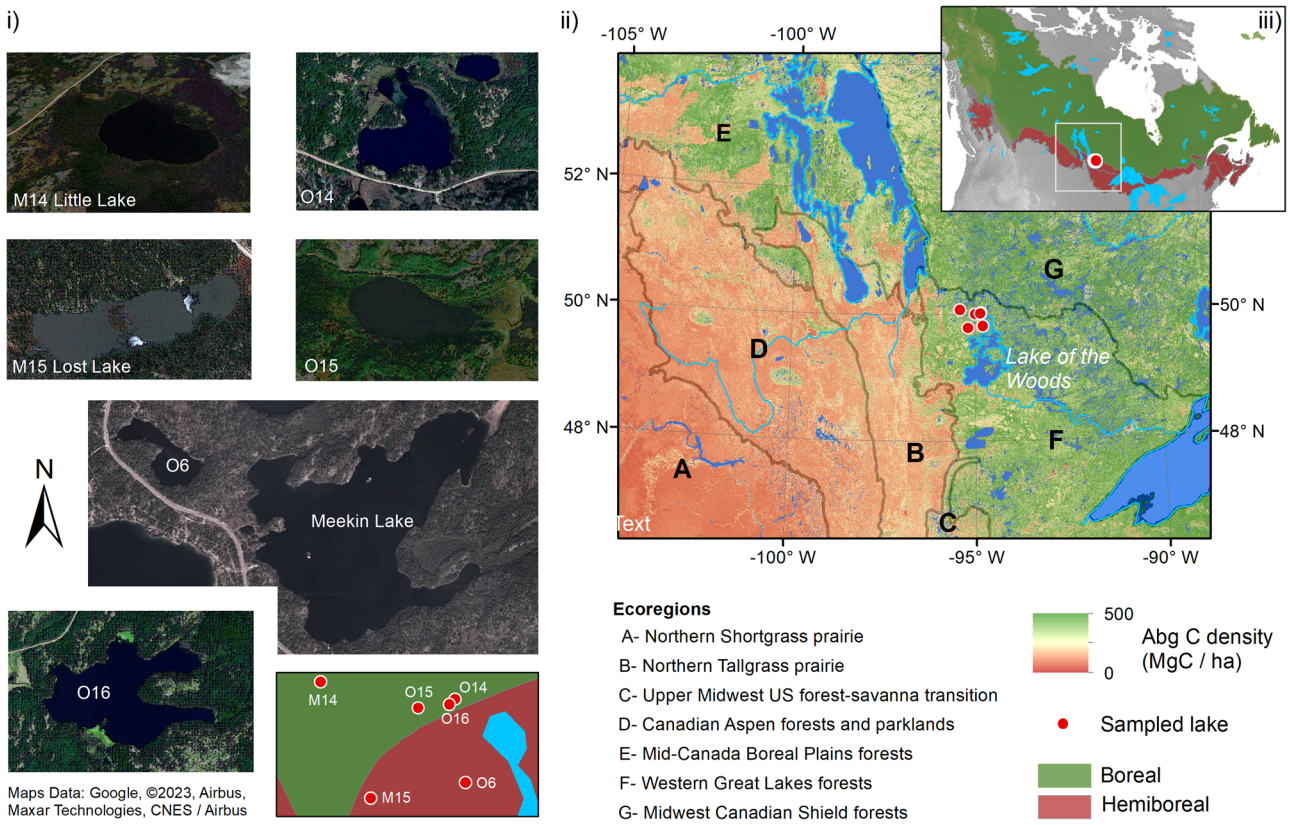

Fig. 1 | Overview of the study area. The six studied lakes (i) and terrestrial ecoregions (ii) forming the prairie-forest ecotone[2]. The sampled lakes are situated to the north of Lake of the Woods, within an area known in Canada as the Lake of the Woods Ecoregion. The extents of the boreal and hemiboreal zones are illustrated in the inset map at the upper right (iii)[1]. The color scheme on the larger map (ii) shows aboveground carbon density as of 2010[121]. Refer to Table 1 for lake coordinates and sizes. Map created using ArcGIS v10.5.1 for Windows.

Livingstone-type sediment cores, Table 1). Ages at the bottom of the cores reached more than 10,000 calibrated years before the present (cal. yrs. BP, i.e., CE 1950) for lakes M15, O6, O14, and O16. Most lakes had relatively stable sedimentation rates during the last 12,000 years as determined from age-depth models (Supplementary Fig. 1). Sedimentation rates varied between 0.03 (M14) to 0.06 cm/yr (O16) (Table 1). Median time intervals between pollen subsamples ranged from 164 years (M15) to 280 years (Meekin) (Table 1).

Historical wildfire activity

Mean regional biomass burning (RegBB), as inferred from pooled ^{14}C- and ^{210}Pb-dated lacustrine charcoal records, displayed episodes of persistent

Table 1 | Characteristics of the six sampled lakes in Ontario and Manitoba

Lake	Latitude (N)	Longitude (W)	Elev.[a] (m)	Max. depth[b] (m)	Lake area (ha)	LS (KB) core length[c] (cm)	Relief	General moisture	Sed. Rate[d] (cm/yr)	Age[e] (cal. yrs. BP)	Pollen[f] (yrs)
M14	50°04'32"	95°24'08"	330	1.2	8.6	247 (51)	Low	Hydric	0.03	9068	—
M15	49°47'09"	95°11'25"	337	5.7	5.3	769 (41)	Med	Xeric	0.05	13,564	172
O6	49°49'17"	94°47'01"	361	3.3	6.3	662 (43)	Med	Xeric	0.05	12,630	280
O14	50°01'42"	94°49'28"	332	8.3	7.0	519 (35)	Med	Xeric	0.04	11,980	—
O15	50°00'29"	94°58'57"	339	3.9	6.2	670 (22)	High	Xeric-mesic	0.05	12,581	164
O16	50°01'07"	94°51'03"	337	3.2	23.0	818 (21)	High	Xeric	0.06	13,088	—

The location, physical features of the lakes, and the general condition of the surrounding landscape are included. The "Relief" column provides an overview of the topography, ranging from low-lying areas surrounded by low-elevation rock outcrops (Low) to lakes bordered by steep outcrops and extensive undulating terrain (High).
[a] Elevation.
[b] Maximum water depth.
[c] Livingstone-type (LS) and Kajak-Brinkhurst (KB) core lengths.
[d] Mean sedimentation rate (mean sample deposition is obtained from its inverse).
[e] Age of the bottom of the core in calibrated years BP.
[f] Median time interval between pollen subsamples.

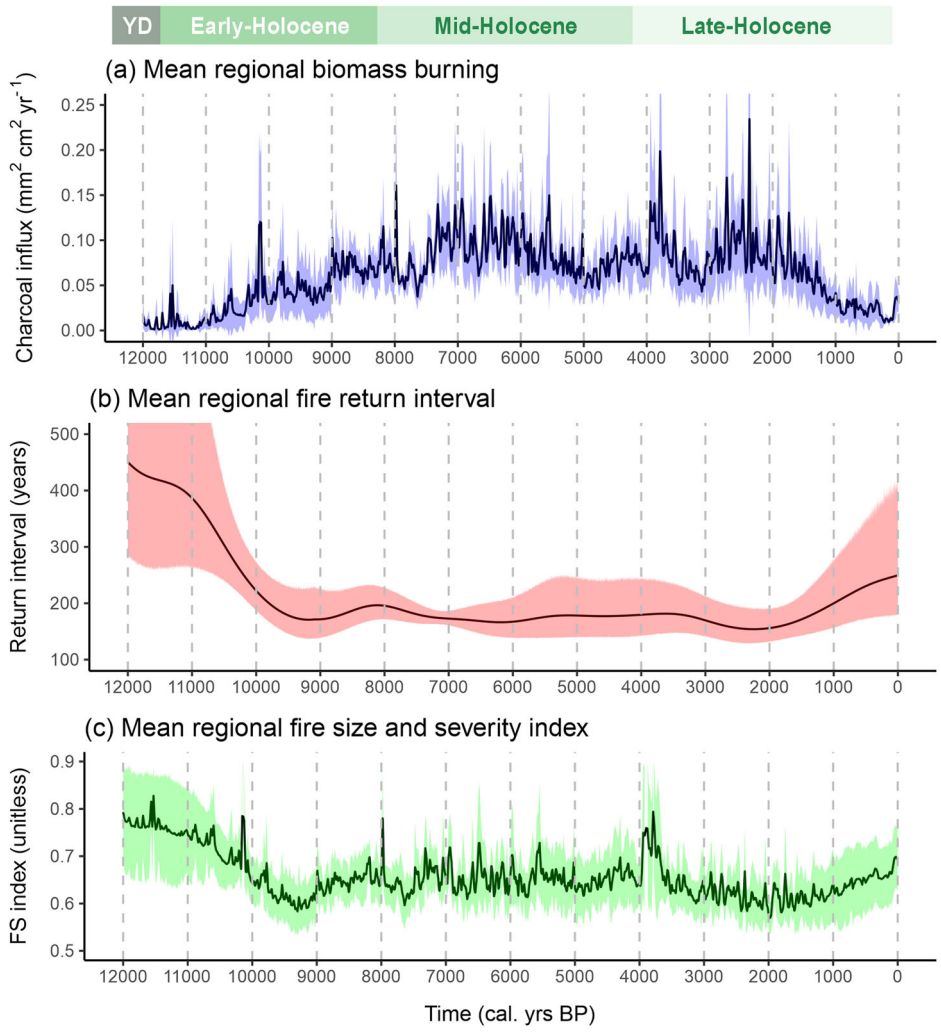

Fig. 2 | Regional fire history. Mean regional **a** biomass burned (RegBB) and **b** fire return interval (RegFRI) for the last 12,000 years, interpolated from charcoal accumulation rates for the six lakes, with 90% CI. Panel **c** represents the mean regional fire size and severity index (RegFS). Sub-epochs of the Holocene epoch (Younger Dryas (YD), early-, mid-, and late-Holocene) are delineated[122].

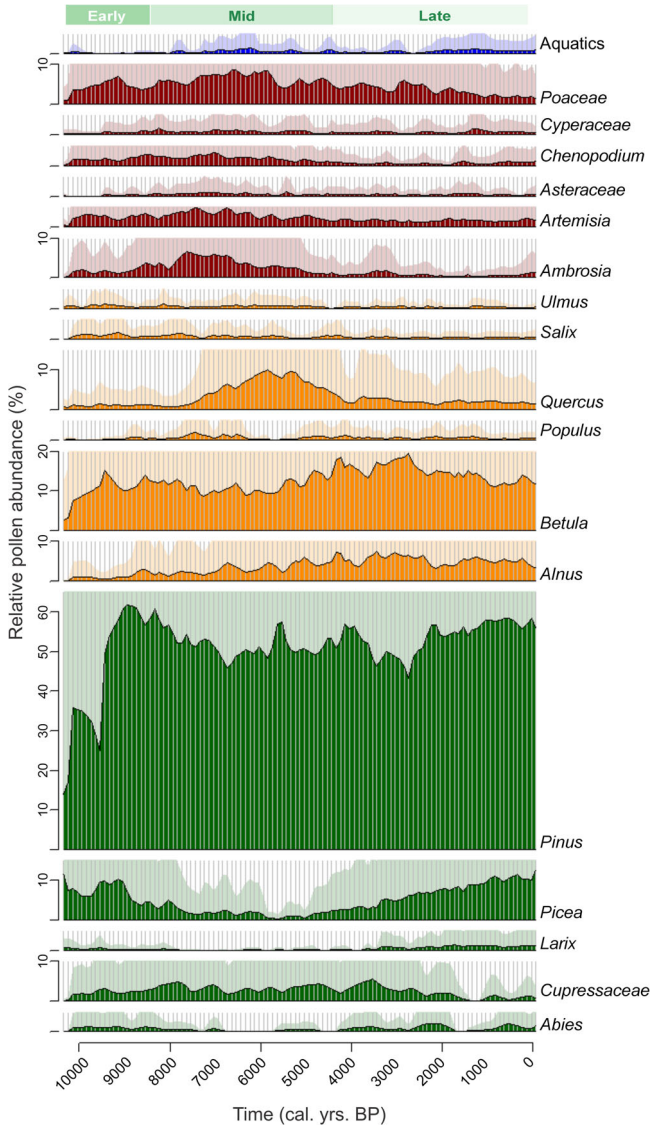

Fig. 3 | Regional vegetation changes. Mean regional relative pollen abundances (%) for the main taxa or families computed from lakes M15, O15 and O6 (Meekin Lake): conifers (green), deciduous trees (orange), shrubs and herbaceous plants (red) and aquatic plants (blue) (see Supplementary Figs. 4 and 5 for data of individual lakes). Pale areas represent five times exaggeration. Sub-epochs of the Holocene epoch (early-, mid- and late-Holocene) are delineated[122]. Gray horizontal lines are equally spaced 100-yrs. intervals for visualization.

elevated activity over the course of the past 12,000 years (Fig. 2a). The lengths of these episodes varied but were on the order of 1000–2000 years. Notably high levels of regional biomass burning occurred around 7200 cal. yrs. BP, 5750 cal. yrs. BP, 4000 cal. yrs. BP, and 2500–1500 cal. yrs. BP. In contrast, regional biomass burning was relatively low before 10,000 cal. yrs. BP, at 3000 cal. yrs. BP, and during the last 1000 years. Charcoal influx during the last 1000 years was significantly lower compared to the preceding 8000 years. Examination of individual site records indicated fluctuations in the level of biomass burning at many sites, although not necessarily in phase (Supplementary Figs. 2 and 3). It was particularly pronounced at Lakes M15 and O15, whereas fire activity elsewhere tended to be more irregular or clustered within specific time periods (Supplementary Fig. 2). The low charcoal influxes observed in recent centuries in Lakes M14, O16, and O6 likely contributed to the simultaneous decline in regional biomass burning.

The trajectory of mean regional fire return intervals (RegFRI), as deduced from charcoal peaks, can be described in three distinct phases. During the early-Holocene, mean fire return intervals shortened gradually, from 400 years to 11,000 cal. yrs. BP to below 200 years at 7000 cal. yrs. BP (Fig. 2b). Throughout the mid-Holocene, mean return intervals between fires among the six lakes were consistently below 180 years (Fig. 2b). In the late-Holocene, the number of recorded fire events decreased, with mean fire return intervals reaching above 250 years. Lakes M14, O15, O6, O14, and O16 all experienced a reduction in recorded fire events during the late-Holocene (Supplementary Fig. 3).

The regional mean fire size and severity metric (RegFF) remained relatively stable throughout the entire period, except possibly during the early-Holocene and toward the present period. During the early period, the metric consistently registered significantly higher values compared to the mid-Holocene (Fig. 2c), indicating a pattern of less frequent but larger and more severe fires during this period. The fire size and severity metric displays an upward trajectory over the last 2000 years, with present levels markedly surpassing the minima observed at 2000 cal. yrs. BP.

Vegetation history

During the early-Holocene, the regional mean pollen record was dominated by pollen from *Pinus* (predominantly *P. banksiana*), *Picea* (undifferentiated), and *Betula*, indicating the presence of a closed-type mixed boreal forest (Fig. 3 and Supplementary Fig. 4). From 8000 to 7000 cal. yrs. BP, there was a transition characterized by a decrease in the relative abundances of boreal taxa and an increase in *Ambrosia*, other non-arboreal pollen (NAP), and *Quercus*. This *Quercus*-NAP phase persisted for approximately a thousand years, followed by the emergence of an oak-pine barren type of ecosystem (*Pinus*, *Quercus*, *Poaceae*, *Artemisia*), which lasted for around 2000 years before reverting to the boreal type around 4000 years cal. yrs. BP. These phases of vegetation development were observed in all three lakes (M15, O15, and Meekin) analyzed for pollen (Fig. 3).

Changes in simulated climate

Climate variability is documented by paleoclimate model simulations spanning the past 12,000 years. Mean annual temperature gradually increased between 12,000- and 10,000-years cal. yrs. BP, following the last glacial period (Fig. 4). The warming trend, which intensified around 7500 cal. yrs. BP with a relatively steeper slope ($+0.11^{\circ}$C per century), persisted until approximately 7000 cal. yrs. BP. Following this period, temperatures stabilized at warmer levels compared to the preceding era. Summer precipitation during the early-Holocene was estimated to be lower than the 5000-3000 cal. yrs. BP mean (Fig. 4). From approximately 7500 to 4000 cal. yrs. BP, the mean annual temperature remained relatively stable, with minor fluctuations. Summer temperatures were estimated to be warmer than the average between 5000 and 3000 cal. yrs. BP, while winter temperatures remained cooler (Fig. 4). Starting from approximately 3000 cal. yrs. BP to the present, there was a gradual cooling trend in mean summer temperatures and a warming trend in mean winter temperatures, interspersed with smaller-scale fluctuations. No meaningful changes in seasonal precipitation were observed in the simulated data over that time horizon. The past few centuries marked the warming as witnessed in observational records.

Human population history

Analysis of archeological radiocarbon dates suggests that human presence in the study area extends to 12,000 − 11,000 cal. yrs. BP (Fig. 4d). During the period from 10,000 to 4000 cal. yrs. BP, population size was low and underwent no substantial long-term change. There may have been an initial population rise between 11,000 and approximately 8000 cal. yrs. BP, followed by a period of population stability until 4200 cal. yrs. BP (Supplementary Fig. 6). However, few dates are available for this period, and overall, the population remained low with minimal long-term growth. Subsequently, there was a population increase between 4000 and approximately 2600 cal. yrs. BP, which was then followed by a slight decrease until around 2200 cal. yrs. BP. Starting from 2200 cal. yrs. BP until 650 cal. yrs. BP, there was a major population increase, followed by a subsequent decrease.

Relationships among fire, climate, vegetation, and human population levels

We investigated the relationships among fire metrics, human population size, relative abundances of pollen genera, and annual mean temperature data over the past 10,000 years (Fig. 5). Relative pollen abundance revealed a clear correlation with centennial to millennial-scale temperature variations. Notably, we observed negative correlations between temperature fluctuations and the abundance of *Picea* (Spearman rho (r_s) = −0.85, *N* bins (N_b) = 200, $p < 0.001$) and *Larix* ($r_s = -0.73$, $N_b = 200$, $p < 0.001$) pollen, while positive correlations were evident for *Quercus* ($r_s = 0.73$, $N_b = 200$, $p < 0.001$), *Poaceae* ($r_s = 0.73$, $N_b = 200$, $p < 0.001$), *Alnus* ($r_s = 0.33$, $N_b = 200$, $p < 0.001$), *Ambrosia* ($r_s = 0.51$, $N_b = 200$, $p < 0.001$), *Artemisia* ($r_s = 0.37$, $N_b = 200$, $p < 0.001$), *Asteraceae* ($r_s = 0.49$, $N_b = 200$, $p < 0.001$), and *Cupressaceae* (*Juniperus* and *Thuja*; $r_s = 0.53$, $N_b = 200$, $p < 0.001$) (where *p* accounted for temporal autocorrelation). Fire metrics (RegBB, RegFRI, and RegFS) showed significant correlations with species abundance and temperature data. Specifically, RegBB exhibited negative correlations with *Larix* ($r_s = -0.52$, $N_b = 103$, $p < 0.001$) and *Picea* ($r_s = -0.57$, $N_b = 103$, $p < 0.001$) but positive correlations with annual temperature ($r_s = 0.62$, $N_b = 1000$, $p < 0.001$) and *Poaceae* ($r_s = 0.69$, $N_b = 103$, $p < 0.001$), *Quercus* ($r_s = 0.45$, $N_b = 103$, $p < 0.001$) and *Cupressaceae* ($r_s = 0.39$, $N_b = 103$, $p < 0.001$). Notably, RegBB closely tracked both short- and long-term fluctuations in *Picea* and *Poaceae* pollen abundances (Fig. 6). Pairwise correlation tests indicated significant positive relationships between RegFRI and *Larix* ($r_s = 0.25$, $N_b = 103$, $p = 0.012$), *Picea* ($r_s = 0.38$, $N_b = 103$, $p < 0.001$), and *Pinus* ($r_s = 0.40$, $N_b = 103$, $p < 0.001$), and negative ones with *Quercus* ($r_s = -0.46$, $N_b = 103$, $p < 0.001$) and *Poaceae* ($r_s = -0.58$, $N_b = 103$, $p < 0.001$). There are also significant correlations between human population size and fire metrics RegBB ($r_s = -0.32$, $N_b = 201$, $p < 0.001$), RegFRI ($r_s = 0.24$, $N_b = 201$, $p < 0.001$) and RegFS ($r_s = -0.33$, $N_b = 201$, $p < 0.001$) (Fig. 5 and Supplementary Figs. 7 and 8). Population sizes tended to increase during periods with longer fire return intervals and decrease during periods of active fire activity.

Discussion

We provided a comprehensive analysis of millennial-scale historical wildfire, vegetation, climate, and human population size dynamics at the prairie-forest ecotone within the hemi-boreal zone in North America. Our study sheds light on the long-term historical dynamics of this nexus, providing valuable insights into the interplay of human presence, climate variability, and natural processes shaping the prairie-forest ecotone.

Climate, vegetation and fire dynamics in the prairie-forest ecotone

Through retrospective analysis of historical ecosystem transformations, we gain valuable insights into potential trajectories for ecosystems amongst prevailing environmental changes. Increasing temperature and aridity are anticipated to affect the distribution and growth of many species, leading to potential changes in the forest structure and composition in this transitional zone[38,39]. Notably, temperature is identified as a key factor driving trends in fire weather within ecosystems surrounding the prairie-forest ecotone, with changes in relative humidity, wind speed, or precipitation playing relatively minor roles[40]. Comparing historical data, the highest rate of temperature change observed in the paleoclimate context was +0.11 °C per century around 7500 years before present. However, current projections suggest a much higher expected rate of change, ranging from +0.31 to +0.47 °C per decade from 1976–2005 to 2051–2080[41]. In response to climate change, there is an expectation that the prairie-forest ecotone may shift northeastward, accompanied by an increase in disturbances such as wildfires, potentially leading to a reduction in the extent of the boreal forest[38,42–44]. Our results provide compelling evidence of such a warming driven shift in vegetation approximately 7000 years before present, characterized by a conversion from a boreal to an oak-pine barrens ecosystem. This unique ecosystem is characterized by its dependence on fire and comprises a savanna community dominated by oak and pine trees, with a canopy cover ranging from a sparse, scattered canopy (5 to 30% cover) to a more closed one (30 to 80%)[45]. The ground layer, predominantly composed of graminoid vegetation, harbors plant species associated with both prairie and forest environments. In contemporary times, this distinctive ecosystem is predominantly located about 300 km south of the study area (identified by the ecoregion labeled as C in Fig. 1). This ecosystem transition persisted for about 2000 years before reverting to a boreal-type ecosystem. The presence of the oak-pine barrens ecosystem coincides with a significant increase of biomass burning (RegBB) and shorter fire return intervals (RegFRI), indicating a clear interplay among ecosystem types and wildfire dynamics in this region[12,38].

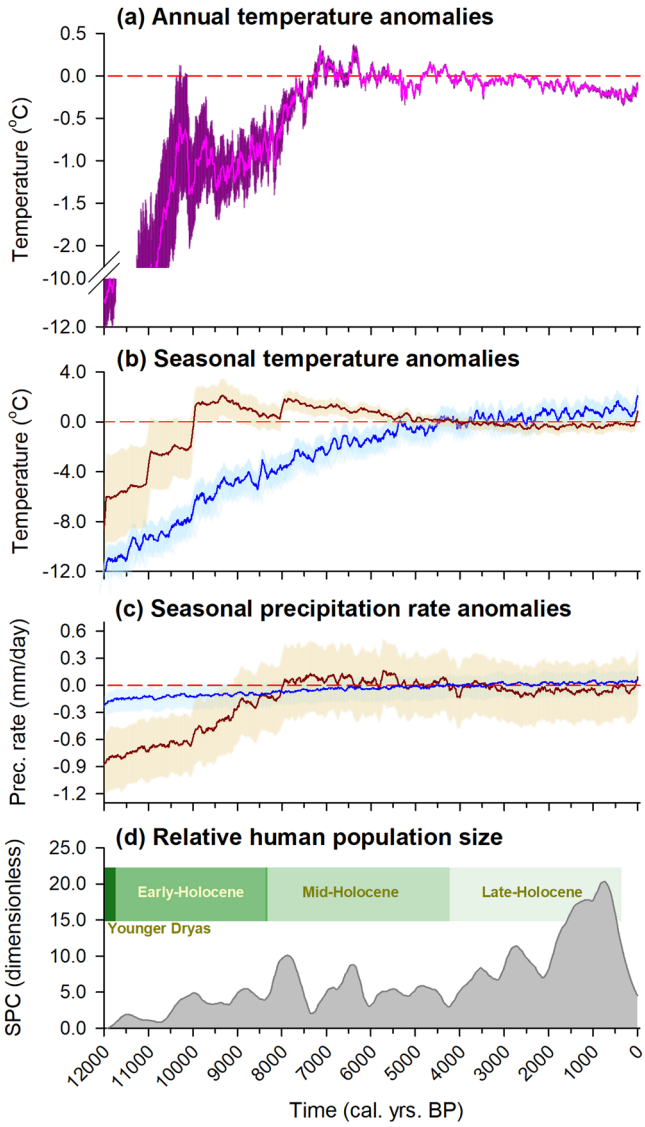

Fig. 4 | Holocene climatic changes and human occupation. (**a**-**c**) Reconstructed mean regional annual (purple), winter (blue) and summer (dark red) temperatures and precipitation rates during the past 12,000 years. Anomalies are shown relative to the mean of 3000-5000 cal. yrs. BP. Shaded area represents 90% confidence interval for the distribution of individual grid cells ($n = 12$). Annual mean temperature (a) was derived from ensemble climate model assimilation of oceanic and terrestrial data from the Temperature 12k proxy database[110]. Seasonal temperature (b) and precipitation rate (c) changes were obtained from outputs of TraCE-21ka-II[111]. (d) Summed probability distribution for relative human population size inferred from archeological data. For this study, we obtained archeological radiocarbon dates for the domain 100W-90W and 45N-55N from CARD 2.0[113] (database downloaded in July 2022), and P3K14C[114] (downloaded in June 2022). Our analysis is truncated during the European Period due to challenges in estimating post-European population trends using this method.

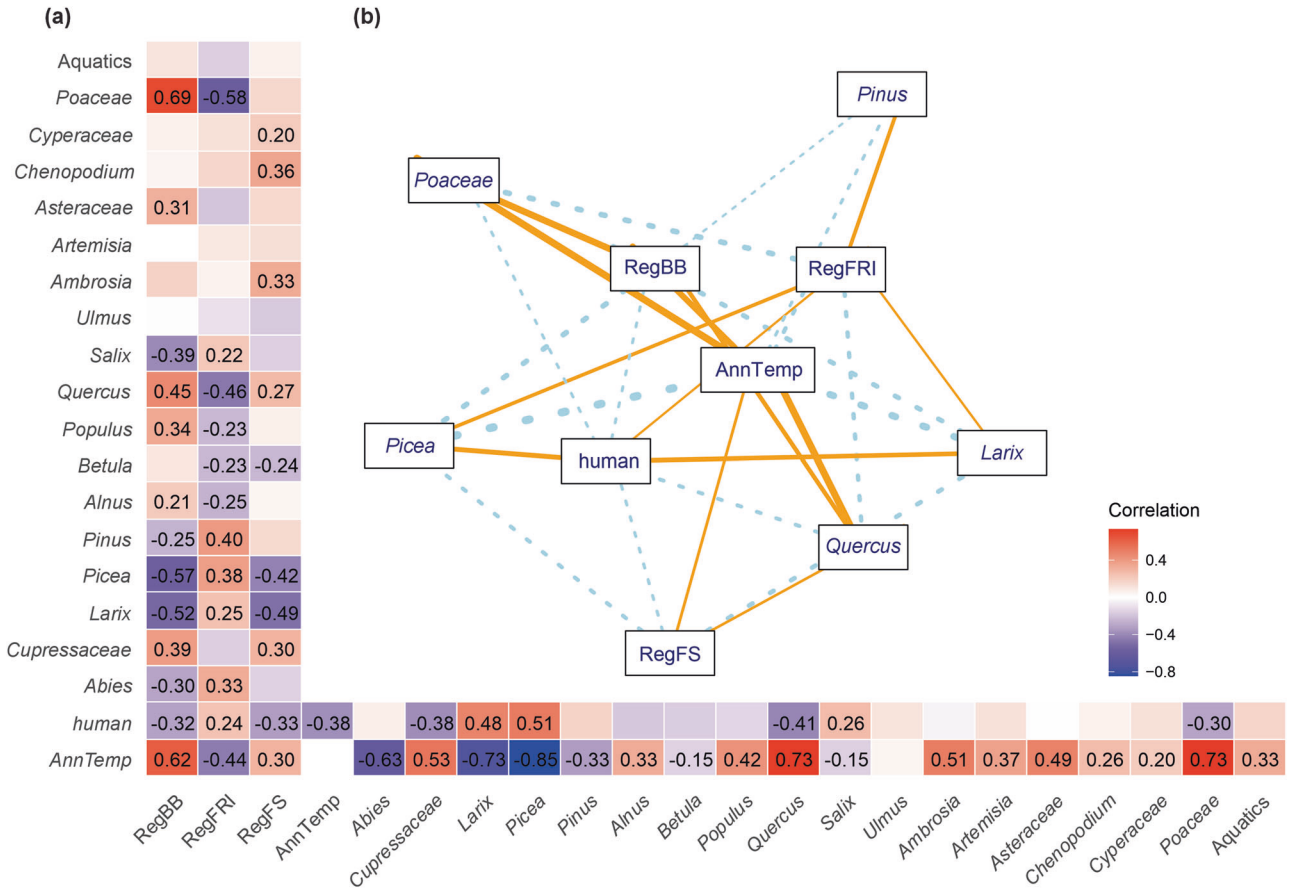

Fig. 5 | Relationships among fire, climate, vegetation, and human population levels. (a) Pairwise correlation heatmap for the relationships among regional human population size, temperature (AnnTemp), relative pollen abundances, and biomass burning, fire return intervals and fire size. Significant correlation coefficients are identified by their rho values. (b) Entity relationship diagram representing significant pairwise correlations ($p < 0.05$) among time series variables. For simplicity, the diagram was limited to *Larix*, *Picea*, *Pinus*, *Poaceae*, and *Quercus* genera. Rectangular boxes depict variables, and lines connect them based on the correlation coefficients. Solid lines indicate positive correlations, while dashed lines indicate negative correlations. Line thickness reflects the magnitude of correlation coefficients. The period of analysis was set to 10,000 cal. yrs. BP to present.

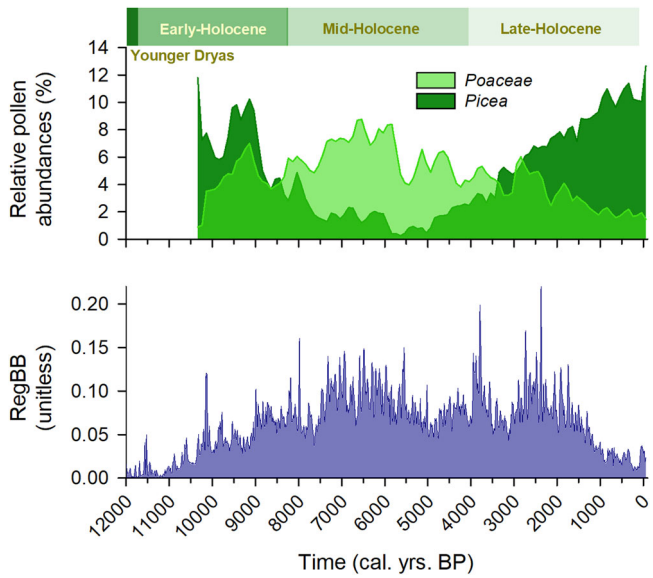

Fig. 6 | Regional biomass burning amidst of *Picea* and *Poaceae*. Regional means of biomass burning (RegBB) and relative pollen abundances (%) for *Poaceae* and *Picea* taxon.

The wildfire trajectories observed in our study region exhibit distinct patterns when compared with surrounding regions. In the context of the broader geographical area, our findings highlight significant variations in fire dynamics over time. During the early-Holocene, the study area exhibited twice as much burning, shifting from a mean fire return interval of approximately 400 years at 11,000 cal. yrs. BP to less than 200 years by 7000 cal. yrs. BP. Progressing to the mid-Holocene fire return intervals were consistently below 180 years. This transition coincides with simulated maximum annual temperatures, although model simulations suggest summers had been warmer for at least 3000 years before this transition. The interpretation of a dry mid-Holocene interpreted from the eastward movement of the prairie-forest border is quite robust[46–50]. In the late-Holocene, the study area witnessed a decline in recorded fire frequency, along with cooling, leading to fire return intervals of around 250 years. This transition stands in contrast to earlier periods and mirrors a fire activity shift akin to the one reconstructed for northeastern boreal coniferous forests[51,52]. This shift from the Holocene climatic optimum to the Neoglacial period was driven by changing orbital forcing and incoming seasonal solar radiation[53], with no apparent alterations observed in vegetation composition[54]. However, the mid- to late-Holocene fire trajectory distinctly diverges when compared to eastern boreal mixed forests. In these forests, fire return intervals generally remained relatively stable over the past 8,000 years[55,56]. The Neoglacial period led to a densification of fire-prone coniferous species therein (at the expense of hardwood cover), contributing to increased fuel availability and offsetting the reduction in fire-conducive weather[54,55,57].

Because coniferous stands are characterized by lower leaf moisture and higher flammability and rate of fire ignition than hardwood stands, their densification may have contributed to an increase of the intensity (i.e., energy output) and rate of spread of fires through the late-Holocene. In the Lake of the Woods Ecoregion, alterations in vegetation observed at the ecotone likely have not played a key role in fluctuations of fire return intervals. However, they may have facilitated larger and more severe fires over the past 3000 years by alleviating the constraints related to fuel scarcity, which would have characterized the Holocene climatic optimum period in this region.

Beside the long-term trajectories, our investigation has unveiled a notable and recurrent pattern of regional biomass burning, distinguished by episodes of persistent elevated activity across a substantial portion of the studied timeframe. These episodes mirror the fluctuations in relative pollen abundance of *Picea* (decreasing with RegBB) and *Poaceae* (increasing with RegBB) (Fig. 6)[58]. This pattern could indicate either a fire regime limited by fuel availability[59,60], where increases and decreases in biomass burning would parallel the fluctuations in fuels, or an oscillatory behavior in synoptic-scale fire-conducive climate conditions[61]. As many of these episodes were asynchronous among sites (Supplementary Fig. 3), the climate hypothesis is less likely as such would imply simultaneous burning across multiple watersheds. Still, the interaction between biomass burning and pollen abundances, particularly during warmer periods with shorter fire return intervals, suggests a nuanced interplay. In the context of climate change during the Holocene sub-epochs, the highs and lows in biomass burning, coupled with taxon-specific pollen abundances, hint at the potential influence of fuel limitation on overall fire severity. This implies that, alongside climatic conditions, fuel availability will play a crucial role in shaping the fire regime dynamics within the study area.

Human population dynamics and landscape interactions

While our results indicate no regional-scale association between human population size and vegetation, population generally increased when regional biomass burning decreased and human population size decreased with increases in *Quercus* pollen. One possible explanation for the correlation between higher population and reduced fire activity is that the low-level burning utilized by the Indigenous peoples in this region for a variety of land management purposes mitigated the risks of larger fires[62,63]. Some authors have suggested that these low-intensity surface fires may not be documented in lake sediments[64]. This recognized limitation[65] could potentially account for the observed absence of significant differences in RegFRI during the transitions from boreal to oak-pine barrens ecosystems during the mid-Holocene. Nevertheless, it is essential to acknowledge another potential limitation related to our understanding of historical fire regimes. The overall sample size of archeological radiocarbon dates was low, although adhering to the sufficiency criteria outlined by Williams[66], and therefore caution is warranted in any interpretation, particularly in the early- and mid-Holocene periods. Records dating between 12,000 and 4000 cal. yrs. BP, constituting two-thirds of the record, are limited to only 112 data points. To gain broader insights, our findings can be juxtaposed with regional analyses both to the north and south of our study area[21,67]. In the southern Midwest, the population remained relatively stable until approximately 4000 years ago, initiating a prolonged increase afterward, with acceleration around 2000 cal. yrs. BP synchronous with decreasing RegFF and RegBB[21]. The adoption of maize agriculture may have contributed to the population increase in the Midwest in the past 1000 years, although the increase in population predates the evidence of maize use in the northern Great Plains. The major area of maize cultivation is to the south of the present-day US-Canadian border[68], but there is evidence of its use, along with that of wild rice into the boreal forest during the past millennium and perhaps earlier[69]. Although there is evidence of cultivation of maize and other crops in Manitoba in the last millennium[70,71], any horticulture was local only and much of the maize may have been obtained by trade[72]. In this region, therefore, there is little evidence to suggest an association between population size and fire regime.

Interestingly, even the slight decrease in the prairie-forest ecotone population size observed between 2600- and 2200-cal. yrs. BP aligns with trends in the southern region[21]. Turning northwards, the Southwest Subarctic region encompasses the boreal forest spanning Ontario to Alberta, making direct comparisons challenging. However, an analogous increase in occupation around 2000 cal. yrs. BP is evident[67]. This population dynamic is intriguingly characterized by a final decrease predating European arrival, echoing trends observed in other regions during the transition from the Medieval Warm Period to the Little Ice Age[21]. However, pinpointing the exact commencement of this decline is difficult due to the smoothing factor and radiocarbon anomalies around that era. Our analysis is truncated during the European Period due to challenges in estimating post-European population trends using this method. Radiocarbon dating is less frequently employed during this period, particularly for deposits left by Indigenous peoples immediately underlying European layers, where historical objects and relative dating methods are more common.

Paleoenvironmental data provide valuable insights for comprehending historical wildfire regimes, including the frequency and severity of past wildfires, and concurrent vegetation and human population dynamics. These reconstructions play a pivotal role in elucidating factors that control vegetation types, range shifts, biogeochemical cycling, and measuring and quantifying ecological resilience under rapid climate change[73]. Moreover, integrating these findings into adaptation and mitigation strategies to the impacts of climate changes holds significance in ensuring sustainable well-being, and more crucially, adaptation[74,75]. Paleoenvironmental data also contribute insights into risks, taking for example, the knowledge gained from paleo-hydrological reconstructions informing flood vulnerability assessments[76] or from paleoseismology for the recurrence intervals of earthquakes[77]. The fire community and society could derive valuable insights from paleoenvironmental sources, aiding in the development of informed decisions regarding fire management, ecological conservation, and community resilience in the face of changing climate or environmental conditions[73,78]. Our findings indicate that open-landscape mosaics, characterized by short-interval fire regimes, represent the natural state for the Lake of the Woods Ecoregion in a warmer climate context than present. Episodes of biomass burning during the mid-Holocene sub-epoch, synchronous with fire-prone boreal coniferous pollen fluctuations, suggest an intensification of fire activity during warm climate settings, particularly when coupled with a substantial biomass and fuel presence. This assumes even greater importance given the area's current low wildfire activity resulting primarily from cooling during the mid- to late-Holocene, allowing for the development of dense forests[75,78]. In the long-term, increasing aridity and a rise in wildfire disturbances anticipated with climate change will reduce the southern extent of the boreal forest[38,79], similar to changes experienced approximately 7000 years before present. At that time, the climate was warmer than present and open grasslands expanded within the hemi-boreal zone. This environmental shift posed substantial challenges for the Indigenous societies inhabiting the prairie-forest ecotone[80]. Consequently, the implementation of preventive measures is imperative to mitigate adverse outcomes. Such measures may encompass regulating human activities like logging and land-use modifications. Concurrently, the development of more efficient firefighting strategies, including controlled burns and fuel reduction practices, remains indispensable in anticipation of the impacts of climate changes in this region[60,75].

Methods

Study area

The Lake of the Woods Ecoregion occupies the southernmost portion of the central Boreal Shield Ecozone[81] (Fig. 1). During the last glaciation, the entirety of the ecoregion was extensively covered by glaciers until around 12,000 years ago[82,83]. The area was subsequently submerged under proglacial Lake Agassiz, which drained approximately 8200 cal. yrs. BP (uncertainties persist regarding the chronology of drainage and the specific locations of outlets)[84,85]. The geology of the ecoregion is primarily composed of massive crystalline Archean rocks and limestone[81,86,87]. The bedrock is covered by

thick to thin glacial till, fluvioglacial, and glacial Lake Agassiz deposits[81,86,87]. The topography is characterized by undulating terrain that alternates between upland bedrock outcrops and lowlands around 300 to 400 m.a.s.l. (above sea level)[81].

The climate of the Lake of the Woods Ecoregion is characterized by cold, long winters and short, warm summers[81,86,87]. The highest mean July temperature for Indian Bay (Manitoba: 49.63° N, 95.12° W) and Kenora (Ontario: 49.78° N, 94.45° W) ranged from 19.1 °C to 19.7 °C, respectively, and the lowest mean January temperature ranged from −17 °C to −16 °C between 1981 to 2010[88]. For the same period, mean total annual precipitation was recorded to be between 630 millimeters (mm) at Indian Bay and 715 mm at Kenora, of which around 536 mm falls as rain[88].

The dominant tree species in the Lake of the Woods Ecoregion include black spruce (*Picea mariana* (Mill.) BSP), jack pine (*Pinus banksiana* Lamb.), white spruce (*Picea glauca* (Moench) Voss), northern white-cedar (*Thuja occidentalis* L.), balsam fir (*Abies balsamea* (L.) Mill), trembling aspen (*Populus tremuloides* Michx.), paper birch (*Betula papyrifera* March), and other hardwoods[81,86,87]. This area also marks the northwestern boundary of the continuous distribution of red pine (*Pinus resinosa* Ait.) and eastern white pine (*Pinus strobus* L.)[89].

Lake selection and sampling

Selection of lakes followed a previous study in which the fire history of the past two millennia was reconstructed for eight watersheds of the Lake of the Woods Ecoregion using a multi-proxy approach combining modern fire statistics, stand initiation maps, tree fire scars, and lake-sedimentary charcoal records[78]. Of these eight lakes, five were selected for further sampling and to reconstruct Holocene fire and vegetation histories: M14, M15, O4, O14, and O15; a sixth lake, O16, was also added (Fig. 1 and Table 1). Sampled lakes had no inflowing streams, a minimum water depth of 1.2 m, no evidence of aquatic plant growth at the center, and minimal evidence of beaver activity. Sediment cores were extracted from the deepest point in each lake from the frozen lake surface in winter 2012. Overlapping 1-m sediment cores were collected using a Livingston-type piston corer[90]. The sediment was wrapped in polyurethane and aluminum foil and transported to the laboratory, where it was stored at 4 °C for conservation. The sediment cores were then sliced into disks at contiguous 1-cm intervals. A Kajak-Brinkhurst (KB) gravity sediment corer[91] was used to collect the most recently deposited material at the water-sediment interface, and it was extruded on site in 1.0-cm segments.

Age-depth models

To establish an age-depth model for surface sediments, the uppermost 1-20 cm of the sediment cores underwent ^{210}Pb measurements. The ^{210}Pb values (listed in Supplementary Table S1) were estimated by measuring the activity of the daughter product, ^{210}Pb, through alpha spectrometry, assuming an equivalent concentration between the two isotopes. The ^{210}Pb concentrations were evaluated using the constant rate of supply (CRS) model of ^{210}Pb accumulation[92]. As the difference between the concentration of unsupported ^{210}Pb and the background (supported ^{210}Pb) concentration decreases with sample depth, the uncertainty of age estimation increases.

For deeper sediments, we built age-depth models based on radiocarbon dating (Table S1) of terrestrial plant macro-remains (needles, leaves, roots, seeds, wood, and bark) and/or bulk gyttja samples by ^{14}C accelerator mass spectrometry (AMS) and using Bayesian age-modeling with the rbacon' v.3.1.1. R package[93] with the ^{210}Pb and ^{14}C dates. We used the IntCal20 calibration curve for terrestrial northern hemisphere material[94] and generated confidence intervals (CI) around the fit based on the probability distribution of each date. We interpolated ages at contiguous 1-cm depth intervals and all dates were expressed in calibrated years before present where, by convention, the base is CE1950 (cal. yrs. BP)[95,96].

Wildfire history

To conduct charcoal analysis, a 1-cm^3 sub-sample was extracted from each 1-cm sediment slice and soaked in a 3% (NaPO3) solution, then wet-sieved through a 160 µm mesh. Charcoal fragments larger than 160 µm typically result from fire events within 1-30 km of the sampled lake shore, which allows for fire events to be reconstructed at the local scale[97–99]. Images of every charcoal particle on the sieve for each 1-cm^3 of sediment processed were taken at 20X magnification using a Moticam 1080 microscope camera linked to a dissecting microscope connected to a computer equipped with the imaging software Moticam Image Plus 3.0[100]. Charcoal measurements were taken, including count and area, and then combined to obtain the charcoal record per centimeter for each lake. An exploratory analysis of the charcoal data was performed using both charcoal count and area[101]. Since both parameters were highly correlated[78,102], only charcoal area is presented and analyzed.

The charcoal series retrieved from the KB and Livingstone-type sediment cores were integrated into one uninterrupted record for each lake. To achieve this, the pattern of charcoal area and number in the KB and Livingstone-type sediment cores were assessed, and the optimal overlapping position was determined[102]. After determining the necessary shift in the data, the entire length of the KB record was retained since it had more accurate dating through ^{210}Pb measurements, and the Livingstone-type sediment core was adjusted accordingly, with overlapping Livingstone-type data removed, resulting in a merged dataset[78].

To obtain a record of past biomass burning at each study site, raw charcoal data (mm^2 cm^{-3}) were converted to charcoal accumulation rate (CHAR; mm^2 cm^{-2} year^{-1}) and then interpolated ($C_{interpolated}$) using the median sample resolution obtained from sediment chronologies. Using the CHAR series, past biomass burning (BB) was inferred, and fire event dates (peaks) were extracted using established methodology[65,103]. These procedures were conducted using CharAnalysis v.1.1 software[104] (available at https://github.com/phiguera/CharAnalysis). A median age derived from the most recent period generally optimizes the detection of recent fire events. The frequency of fire events (FF; fire.year^{1}) was compiled at each site using a kernel density estimation procedure based on a 500-year smoothing bandwidth[51].

The six individual BB series were pooled into a regional biomass burning history spanning 12,000 cal. yrs. BP to present[51] (hereafter RegBB; unitless). Similarly, the frequencies of fire events at each site were averaged into a regional fire frequency record (RegFF). We used the ratio between BB and FF to assess fluctuations in fire size and severity through time for individual and regional records (hereafter RegFS index)[51]. Significance of changes in RegFF, RegBB, and RegFS was evaluated using a bootstrap procedure applied to sites with 999 iterations (BCI; 90%). Changes in these fire metrics are considered significant if the 90% BCI do not overlap between two periods. While RegBB values are correlated with long-term changes in area burned, fire size and severity index are related to the temporal trajectory of mean biomass burned per fire, reflecting part of the loss of organic matter modulated by the number of fires through time. High values of RegFS are indicative of a high mean area burned or severity per fire, whereas low RegFS values may indicate a low mean area burned or severity per fire[51]. Finally, RegFF were converted into mean regional fire return intervals (RegFRI) using the inverse transformation (1/RegFF).

Vegetation history

Using palynological analysis of subsamples of sediment (1 cm^3) taken at 10 cm intervals along the core of lakes M15 (hemiboreal) and O15 (boreal), we reconstructed the Holocene vegetation dynamics. Standard techniques were employed to process, count and identify pollen and spores in sediment subsamples[105]. In each subsample, we counted a minimum of 300 pollen grains of terrestrial taxa using a microscope with a magnification factor of either 200 or 400. Pollen grains were identified based on pollen keys[106,107], with tree pollen identified to the genus level. Pollen and spores of aquatic plants were also identified. To estimate pollen concentration (grains cm^{-3}) and accumulation rate (grains cm^{-2} yr^{-1}), we added exotic marker pollen (*Eucalyptus*) to each subsample.

A previously published vegetation history from Meekin Lake[108] was also used in our analyses; Meekin Lake (hemiboreal) is located 250 meters

west of our sampled lake O6 (Fig. 1). Coring of Meekin Lake, which had a 15 m water column, was made using a Livingston-type sediment corer during summer 2011, for a cumulative core length of ~9m[108]. For pollen analysis, the 1 cm^3 subsamples were taken at regularly intervals of 16 cm[108].

The relative pollen abundance percentages of the dominant trees, shrubs and herbs taxa (> 1.0% for M15 and O15, and > 5.0% for Meekin[108] were computed for each sample for each lake. Relative pollen abundances of aquatic taxa were summed into a single entry. These values were then averaged to create an index of regional vegetation dynamics. In cases where a taxon was absent from a specific sample, it was assigned a value of 0% in the regional computation. The resulting data were plotted using the 'rioja' package in R[109].

Climate dynamics

We used spatially complete outputs of annual mean temperatures covering the past 12,000 years derived from assimilation of oceanic and terrestrial data from the Temperature 12k data with information from transient climate models PMIP4 HadCM3 and TraCE-21ka[110] (https://zenodo.org/record/6426332). We extracted the complete outputs (the average of all simulations) of annual mean temperature, at 10-year time resolution, for the domain of 100°W–90°W and 45°N–55°N, and time span of 12,000 to 0 cal. yrs. BP. We took note of the highest rates of change (°C per century) in this paleoclimate reconstruction. We also analyzed the seasonality of temperature and precipitation rate changes in the study region during the period from 11,700 to 5000 cal. yrs. BP by utilizing the results obtained from the updated version of TraCE-21ka (-II). These simulations include climatic forcing from Earth's orbital variations and greenhouse gases, as well as improvements in the modeling of Atlantic Ocean circulation and its relationship to freshwater from melting polar ice[111] (https://trace-21k.nelson.wisc.edu/Data.html). A 100-year running-average was applied to TraCE-21ka-II reconstructions. All data were expressed as anomalies relative to 5000−3000 cal. yrs. BP (as per Erb et al.[110]).

Human demographic history

Databases of archeological radiocarbon dates have proven to be a valuable tool for estimating past human population sizes[66,112]. This approach uses radiocarbon dates from archeological sites as a proxy for population density[21]. For this study, we obtained archeological radiocarbon dates for the domain 100W-90W and 45N-55N from CARD 2.0[113] (database downloaded in July 2022), and P3K14C[114] (downloaded in June 2022). Where dates were overlapping among databases, the CARD record was retained as it contains more detailed information per record. To ensure data quality, records associated with human activity and dated to less than 50 ka (50,000 cal. yrs. BP) and more than zero were retained, while duplicates, records flagged as anomalous, not associated with an archeological site/human activity (e.g., geochronology and paleobiology dates), containing an error larger than age, from the historic European/post-colonial period, and from human remains were excluded. The final dataset consisted of 762 dates (CARD: 588 and P3K14C: 174). Data were processed as described by the original work[21]. Once radiocarbon dates were calibrated, the summed probability distribution (SPD) curve was generated. Sampling bias was accounted for by binning dates from the same site in 200-year bins; all dates within a bin were combined and treated as a single date in the SPD. Noise induced by the calibration process was remediated by smoothing the SPD using a local regression equivalent to a 500-year running mean[66]. The SPD was then adjusted for loss through time due to taphonomic factors[115].

Numerical analyses

Relationships among mean regional fire metrics (RegBB, RegFRI, RegFS), mean annual temperatures[110], relative pollen abundances, and relative human population size[21] were examined using binned correlation[116]. The approach enables correlation assessments among time-series datasets with dissimilar temporal characteristics, making it particularly useful for analyzing paleoenvironmental data with varying sampling frequencies and temporal resolutions[117,118]. We employed the Spearman rho coefficient, with 95% confidence interval, for quantification of the magnitude of relationships; the bin-widths were estimated for each pairwise comparison considering the persistence (memory) estimated for each unevenly spaced time series. Results were visually depicted using an entity relationship diagram, which is a structural plot containing symbols and connectors that visualize the major entities within ecosystem dynamics, and the inter-relationships among these entities. The investigation period ranged from 10,000 to 0 cal. yrs. BP, with limitations imposed by pollen data extending towards the past and population size data towards the present. Of note is that some correlations may appear counterintuitive, potentially stemming from the use of relative metrics, such as pollen percentages, or arising as a product of two metrics (as is the case with RegFRI). The reader is encouraged to consider the potential influence of such methodological artifacts on the observed associations. Analysis was conducted using the R package BINCOR[116]; the entity relationship diagram was generated using the igraph and ggplot2 packages[119,120].

Data availability

The climate data used to support the findings of this study were obtained from https://zenodo.org/records/6426332 and https://trace−21k.nelson.wisc.edu/Data.html. Charcoal, pollen, and human demographic history data are available on figshare (https://doi.org/10.6084/m9.figshare.25155593.v1).

Code availability

All relevant software and R-functions that support the methods of this study are referred to in the "Methods" section (see package vignettes for details).

Received: 12 December 2023; Accepted: 22 March 2024;
Published online: 03 April 2024

References

1. Brandt, J. P. The extent of the North American boreal zone. *Environ. Rev.* **17**, 101–161 (2009).
2. Dinerstein, E. et al. An ecoregion-based approach to protecting half the terrestrial realm. *BioScience* **67**, 534–545 (2017).
3. Kier, G. et al. Global patterns of plant diversity and floristic knowledge: global plant diversity. *J. Biogeography* **32**, 1107–1116 (2005).
4. Fowler, N. L. & Beckage, B. Savannas of North America. in *Savanna Woody Plants and Large Herbivores* (eds. Scogings, P. F. & Sankaran, M.) 123–150 (Wiley, 2019). https://doi.org/10.1002/9781119081111.ch5.
5. Jenkins, C. N., Pimm, S. L. & Joppa, L. N. Global patterns of terrestrial vertebrate diversity and conservation. *Proc. Natl Acad. Sci. USA* **110**, E2602–E2610 (2013).
6. Jung, M. et al. Areas of global importance for conserving terrestrial biodiversity, carbon and water. *Nat. Ecol. Evol.* **5**, 1499–1509 (2021).
7. Fang, X. et al. *A Review of Canadian Prairie Hydrology: Principles, Modelling and Response to Land Use and Drainage Change* (Centre for Hydrology), 32 (University Saskatchewan, Saskatoon, Saskatchewan, 2007).
8. Millett, B., Johnson, W. C. & Guntenspergen, G. Climate trends of the North American prairie pothole region 1906–2000. *Clim. Change* **93**, 243–267 (2009).
9. Statistics Canada. *Measuring Ecosystem Goods and Services in Canada - Human Activity and the Environment*. https://www150.statcan.gc.ca/n1/pub/16-509-x/2016001/31-eng.htm (2013).
10. Laliberte, A. S. & Ripple, W. J. Range contractions of North American carnivores and ungulates. *BioScience* **54**, 123–138 (2004).
11. Newbold, T. et al. Has land use pushed terrestrial biodiversity beyond the planetary boundary? A global assessment. *Science* **353**, 288–291 (2016).
12. Baltzer, J. L. et al. Increasing fire and the decline of fire adapted black spruce in the boreal forest. *Proc. Natl. Acad. Sci. USA.* **118**, e2024872118 (2021).

13. Ratajczak, Z., Nippert, J. B., Briggs, J. M. & Blair, J. M. Fire dynamics distinguish grasslands, shrublands and woodlands as alternative attractors in the Central Great Plains of North America. *J Ecol* **102**, 1374–1385 (2014).
14. Cruz, M. G., Alexander, M. E. & Kilinc, M. Wildfire rates of spread in grasslands under critical burning conditions. *Fire* **5**, 55 (2022).
15. Cheney, N. P., Gould, J. S. & Catchpole, W. R. Prediction of fire spread in grasslands. *Int. J. Wildland Fire* **8**, 1–13 (1998).
16. Benalcazar, P. et al. The impact of land conversion from boreal forest to agriculture on soil health indicators. *Can. J. Soil. Sci.* **102**, 651–658 (2022).
17. Davis, S. K., Bogard, H. J. K., Kirk, D. A., Moretto, L. & Brigham, R. M. Grassland songbird abundance is influenced more strongly by individual types of disturbances than cumulative disturbances associated with natural gas extraction. *PLOS ONE* **18**, e0283224 (2023).
18. Kurz, W. A. et al. Carbon in Canada's boreal forest — A synthesis. *Environ. Rev.* **21**, 260–292 (2013).
19. Vilà, M. et al. Ecological impacts of invasive alien plants: a meta-analysis of their effects on species, communities and ecosystems. *Ecol. Lett.* **14**, 702–708 (2011).
20. Shaffer, J. A., Roth, C. L. & Mushet, D. M. Modeling effects of crop production, energy development and conservation-grassland loss on avian habitat. *PLOS ONE* **14**, e0198382 (2019).
21. Briere, M. D. & Gajewski, K. Holocene human-environment interactions across the Northern American prairie-forest ecotone. *Anthropocene* **41**, 100367 (2023).
22. Moos, M. T. & Cumming, B. F. Changes in the parkland-boreal forest boundary in northwestern Ontario over the Holocene. *Quat. Sci. Rev.* **30**, 1232–1242 (2011).
23. Bonan, G. B. & Shugart, H. H. Environmental factors and ecological processes in boreal forests. *Annu. Rev. Ecol. Evol. Syst.* **20**, 1–28 (1989).
24. Hogg, E. H. Climate and the southern limit of the western Canadian boreal forest. Can. J. For. Res. 24, 1835–1845 (1994).
25. Nelson, D. M. & Hu, F. S. Patterns and drivers of Holocene vegetational change near the prairie–forest ecotone in Minnesota: revisiting McAndrews' transect. *New Phytol.* **179**, 449–459 (2008).
26. Teed, R., Umbanhower, C. & Camill, P. Multiproxy lake sediment records at the northern and southern boundaries of the Aspen Parkland region of Manitoba. *Canada. Holocene* **19**, 937–948 (2009).
27. Williams, J. W., Shuman, B. & Bartlein, P. J. Rapid responses of the prairie-forest ecotone to early Holocene aridity in mid-continental North America. *Glob. Planet. Change* **66**, 195–207 (2009).
28. Camill, P. et al. Late-glacial and Holocene climatic effects on fire and vegetation dynamics at the prairie–forest ecotone in south-central Minnesota. *J. Ecology* **91**, 822–836 (2003).
29. Lavorel, S., Flannigan, M. D., Lambin, E. F. & Scholes, M. C. Vulnerability of land systems to fire: Interactions among humans, climate, the atmosphere, and ecosystems. *Mitig. Adapt. Strat. Glob. Change* **12**, 33–53 (2006).
30. Oswald, W. W. et al. Conservation implications of limited Native American impacts in pre-contact New England. *Nat. Sustain.* **3**, 241–246 (2020).
31. Roos, C. I., Zedeño, M. N., Hollenback, K. L. & Erlick, M. M. H. Indigenous impacts on North American Great Plains fire regimes of the past millennium. *Proc. Natl. Acad. Sci. USA.* **115**, 8143–8148 (2018).
32. Higgins, K. F. *Interpretation and Compendium of Historical Fire Accounts in the Northern Great Plains*. *Resource Publication* https://pubs.usgs.gov/publication/2000128 (1986).
33. Stewart, Omer. C. *Forgotten Fires*. (Norman, OK, 2002).
34. Delcourt, P. A. & Delcourt, H. R. *Prehistoric Native Americans and Ecological Change: Human Ecosystems in Eastern North America since the Pleistocene*. (Cambridge University Press, Cambridge, 2004). https://doi.org/10.1017/CBO9780511525520.
35. Gajewski, K., Kriesche, B., Chaput, M. A., Kulik, R. & Schmidt, V. Human–vegetation interactions during the Holocene in North America. *Veget. Hist. Archaeobot.* **28**, 635–647 (2019).
36. Munoz, S. E., Mladenoff, D. J., Schroeder, S. & Williams, J. W. Defining the spatial patterns of historical land use associated with the indigenous societies of eastern North America. *J. Biogeography* **41**, 2195–2210 (2014).
37. Roos, C. I. Scale in the study of Indigenous burning. *Nat. Sustain.* **3**, 898–899 (2020).
38. Chaste, E., Girardin, M. P., Kaplan, J. O., Bergeron, Y. & Hély, C. Increases in heat-induced tree mortality could drive reductions of biomass resources in Canada's managed boreal forest. *Landscape Ecol*. https://doi.org/10.1007/s10980-019-00780-4 (2019).
39. McKenney, D. W., Pedlar, J. H., Lawrence, K., Campbell, K. & Hutchinson, M. F. Potential impacts of climate change on the distribution of North American trees. *BioScience* **57**, 939–948 (2007).
40. Jain, P., Castellanos-Acuna, D., Coogan, S. C. P., Abatzoglou, J. T. & Flannigan, M. D. Observed increases in extreme fire weather driven by atmospheric humidity and temperature. *Nat. Clim. Chang.* **12**, 63–70 (2022).
41. Prairie Climate Centre. Climate Change in Canada. *Climate Atlas of Canada* https://climateatlas.ca/home-page (2019).
42. Frelich, L. E. & Reich, P. B. Will environmental changes reinforce the impact of global warming on the prairie–forest border of central North America? *Front. Ecol. Evol.* **8**, 371–378 (2010).
43. Hogg, E. H. & Bernier, P. Y. Climate change impacts on drought-prone forests in western Canada. For. Chron. 81, 675–682 (2005).
44. Karmakar, M., Leavitt, P. R. & Cumming, B. F. Enhanced algal abundance in northwest Ontario (Canada) lakes during the warmer early-to mid-Holocene period. *Quat. Sci. Rev.* **123**, 168–179 (2015).
45. Cohen, J. G. Oak-Pine Barrens - Michigan Natural Features Inventory. Michigan Natural Features Inventory, Michigan State University Extension, Lansing, Michigan. https://mnfi.anr.msu.edu/communities/description/10692 (2000).
46. Holloway, R. & Bryant, V. Late-Quaternary pollen records and vegetational history of the Great Lakes region: United States and Canada. In *Pollen records of late-Quaternary North American sediments* (eds Bryant, V. & Holloway, R.) 205–245 (American Association of Stratigraphic Palynologists Foundation, Dallas, Texas, 1985).
47. Nichols, H. The late quaternary history of vegetation and climate at porcupine mountain and clearwater bog. *Manitoba. Arct. Alp. Res.* **1**, 155 (1969).
48. Ritchie, J. C. & Yarranton, G. A. The late-quaternary history of the boreal forest of Central Canada, based on standard pollen stratigraphy and principal components analysis. *J. Ecol.* **66**, 199 (1978).
49. Shuman, B. N. & Marsicek, J. The structure of Holocene climate change in mid-latitude North America. *Quat. Sci. Rev.* **141**, 38–51 (2016).
50. Webb, T., Bartlein, P., Harrison, S. & Anderson, K. Vegetation, lake levels, and climate in eastern North America for the past 18,000 years. In *Global Climates since the last Glacial Maximum* (eds Wright, H. et al) 415–467 (University of Minnesota Press, Minneapolis, 1993).
51. Ali, A. A. et al. Control of the multimillennial wildfire size in boreal North America by spring climatic conditions. *Proc. Natl. Acad. Sci. USA* **109**, 20966–20970 (2012).
52. Hély, C. et al. Eastern boreal North American wildfire risk of the past 7000 years: A model-data comparison. *Geophys. Res. Lett*. **37**, L14709 (2010).
53. Davis, B. A. S. & Brewer, S. Orbital forcing and role of the latitudinal insolation/temperature gradient. *Clim Dyn* **32**, 143–165 (2009).
54. Blarquez, O. et al. Regional paleofire regimes affected by non-uniform climate, vegetation and human drivers. *Sci. Rep.* **5**, 13356 (2015).

55. Girardin, M. P. et al. Vegetation limits the impact of a warm climate on boreal wildfires. *New. Phytol.* **199**, 1001–1011 (2013).
56. Senici, D., Chen, H. Y. H., Bergeron, Y. & Ali, A. A. The effects of forest fuel connectivity on spatiotemporal dynamics of Holocene fire regimes in the central boreal forest of North America. *J. Quaternary Sci.* **30**, 365–375 (2015).
57. Remy, C. C. et al. Guidelines for the use and interpretation of palaeofire reconstructions based on various archives and proxies. *Quat. Sci. Rev.* **193**, 312–322 (2018).
58. Remy, C. C. et al. Wildfire size alters long-term vegetation trajectories in boreal forests of eastern North America. *J. Biogeogr.* **44**, 1268–1279 (2017).
59. Boulanger, Y. et al. Changes in mean forest age in Canada's forests could limit future increases in area burned but compromise potential harvestable conifer volumes. *Can. J. For. Res.* **47**, 755–764 (2017).
60. Parisien, M.-A. et al. Fire deficit increases wildfire risk for many communities in the Canadian boreal forest. *Nat. Commun.* **11**, 2121 (2020).
61. Girardin, M. P., Tardif, J. & Flannigan, M. D. Temporal variability in area burned for the province of Ontario, Canada, during the past 200 years inferred from tree rings. *J. Geophys. Res.* **111**, D17108 (2006).
62. Kimmerer, R. W. & Lake, F. K. The role of indigenous burning in land management. *J. Forestry* **99**, 36–41 (2001).
63. Miller, A. M. & Davidson-Hunt, I. Fire, agency and scale in the creation of aboriginal cultural landscapes. *Hum. Ecol.* **38**, 401–414 (2010).
64. Abrams, M. D. & Nowacki, G. J. Native American imprint in palaeoecology. *Nat. Sustain.* **3**, 896–897 (2020).
65. Higuera, P. E. et al. Peak detection in sediment–charcoal records: impacts of alternative data analysis methods on fire-history interpretations. *Int. J. Wildland Fire* **19**, 996–1014 (2010).
66. Williams, A. N. The use of summed radiocarbon probability distributions in archaeology: a review of methods. *J. Archaeol. Sci.* **39**, 578–589 (2012).
67. Briere, M. D. & Gajewski, K. Human population dynamics in relation to Holocene climate variability in the North American Arctic and Subarctic. *Quat. Sci. Rev.* **240**, 106370 (2020).
68. Moodie, D. W. & Kaye, B. The northern limit of Indian agriculture in North America. *Geograph. Rev.* **59**, 513–529 (1969).
69. Boyd, M. & Surette, C. Northernmost precontact maize in North America. *Am. Antiq.* **75**, 117–133 (2010).
70. Flynn, C. & Syms, E. L. Manitoba history: Manitoba's first farmers. *Manit. Hist. Soc. Newsl.* **31**, 4–11 (1996).
71. Schneider, F. Prehistoric horticulture in the northeastern plains. *Plains Anthropol.* **47**, 33–50 (2002).
72. Boyd, M., Surette, C. & Nicholson, B. A. Archaeobotanical evidence of prehistoric maize (Zea mays) consumption at the northern edge of the Great Plains. *J. Archaeol. Sci.* **33**, 1129–1140 (2006).
73. Seddon, A. W. R. et al. Looking forward through the past: identification of 50 priority research questions in palaeoecology. *J. Ecol.* **102**, 256–267 (2014).
74. Cyr, D., Gauthier, S., Bergeron, Y. & Carcaillet, C. Forest management is driving the eastern North American boreal forest outside its natural range of variability. *Front. Ecol. Environ.* **7**, 519–524 (2009).
75. Girardin, M. P. et al. Fire in managed forests of eastern Canada: Risks and options. *For. Ecol. Manag.* **294**, 238–249 (2013).
76. Nolin, A. F. et al. Observed and projected trends in spring flood discharges for the Upper Harricana River, eastern boreal Canada. *J. Hydrol. Reg. Stud.* **48**, 101462 (2023).
77. Atwater, B. F. et al. Earthquake recurrence inferred from paleoseismology. in *Developments in Quaternary Sciences* vol. 1 331–350 (Elsevier, 2003).
78. Waito, J. et al. Recent fire activity in the boreal eastern interior of North America is below that of the past 2000 yr. *Ecosphere* **9**, e02287 (2018).
79. Gaboriau, D. M. et al. Interactions within the climate-vegetation-fire nexus may transform 21st century boreal forests in northwestern Canada. *iScience* **26**, 106807 (2023).
80. Meyer, D., Beaudoin, A. & Amundson, L. The Paleo-Indian period. in *Human ecology of the Canadian prairie ecozone* 5–53 (2011).
81. Ecological Stratification Working Group. *A National Ecological Framework for Canada.* https://sis.agr.gc.ca/cansis/publications/manuals/1996/index.html (1996).
82. Dalton, A. S. et al. Deglaciation of the north American ice sheet complex in calendar years based on a comprehensive database of chronological data: NADI−1. *Quat. Sci. Rev.* **321**, 108345 (2023).
83. Dyke, A. Late Quaternary vegetation history of northern North America based on pollen, macrofossil, and faunal remains. *Geograph. Phys. Quatern.* **59**, 211–262 (2005).
84. Murton, J. B., Bateman, M. D., Dallimore, S. R., Teller, J. T. & Yang, Z. Identification of Younger Dryas outburst flood path from Lake Agassiz to the Arctic Ocean. *Nature* **464**, 740–743 (2010).
85. Thorleifson, L. H. Review of Lake Agassiz. in *History.Sedimentology, geomorphology, and history of the central Lake Agassiz Basin, field trip B2., Winnipeg Section* 55–84 (Geological Association of Canada, Winnipeg, Manitoba, Canada., 1996).
86. Crins, W. J., Gray, P. A., Uhlig, P. W. C. & Wester, M. C. *The Ecosystems of Ontario, Part 1: Ecozones and Ecoregions*. (2009).
87. Smith, R. E. et al. *Terrestrial Ecozones, Ecoregions and Ecodistricts of Manitoba*. (1998).
88. GCCN (Government of Canada Climate Normals). 1981-2010 Climate Normals & Averages. https://climate.weather.gc.ca/climate_normals/index_e.html (2016).
89. Wendel, G. W. & Smith, H. C. Eastern white pine. in *Silvics of North America, vol. 1, Conifers. USDA* vol. 654 476–488 (Washington, DC, 1990).
90. Wright, H. E. Jr., Mann, D. H. & Glaser, P. H. Piston Corers for Peat and Lake Sediments. *Ecology* **65**, 657–659 (1984).
91. Glew, J. R., Smol, J. P. & Last, W. M. Sediment core extraction and extrusion. in *Tracking environmental change using lake sediments volume 1: basin analysis, coring and chronological techniques* 7–105 (Kluwer Academic Publishers, Dordrecht, The Netherlands, 2001).
92. Appleby, P. G. & Oldfield, F. The calculation of lead-210 dates assuming a constant rate of supply of unsupported 210Pb to the sediment. *CATENA* **5**, 1–8 (1978).
93. Blaauw, M. & Christen, J. A. Flexible paleoclimate age-depth models using an autoregressive gamma process. *Bayesian Anal.* **6**, 457–474 (2011).
94. Reimer, P. J. et al. The IntCal20 Northern Hemisphere radiocarbon age calibration curve (0–55 cal kBP). *Radiocarbon* **62**, 725–757 (2020).
95. Blaauw, M. Methods and code for 'classical' age-modelling of radiocarbon sequences. *Quat. Geochronol.* **5**, 512–518 (2010).
96. Trachsel, M. & Telford, R. J. All age–depth models are wrong, but are getting better. *Holocene* **27**, 860–869 (2017).
97. Higuera, P. E., Peters, M. E., Brubaker, L. B. & Gavin, D. G. Understanding the origin and analysis of sediment-charcoal records with a simulation model. *Quat. Sci. Rev.* **26**, 1790–1809 (2007).
98. Lynch, J. A., Clark, J. S. & Stocks, B. J. Charcoal production, dispersal, and deposition from the Fort Providence experimental fire: interpreting fire regimes from charcoal records in boreal forests. *Can. J. For. Res.* **34**, 1642–1656 (2004).
99. Oris, F. et al. Charcoal dispersion and deposition in boreal lakes from 3 years of monitoring: Differences between local and regional fires: Monitoring charcoal deposition in lakes. *Geophys. Res. Lett.* **41**, 6743–6752 (2014).
100. Motic Images. Motic Images Plus 3.0 ML Software. Motic Asia (2018).

101. Carcaillet, C., Bouvier, M., Fréchette, B., Larouche, A. C. & Richard, P. J. H. Comparison of pollen-slide and sieving methods in lacustrine charcoal analyses for local and regional fire history. *Holocene* **11**, 467–476 (2001).
102. Ali, A. A., Higuera, P. E., Bergeron, Y. & Carcaillet, C. Comparing fire-history interpretations based on area, number and estimated volume of macroscopic charcoal in lake sediments. *Quat. Res.* **72**, 462–468 (2009).
103. Brossier, B. et al. Using tree-ring records to calibrate peak detection in fire reconstructions based on sedimentary charcoal records. *Holocene* **24**, 635–645 (2014).
104. Higuera, P. E. CharAnalysis 1.1: diagnostic and analytical tools for sediment charcoal analysis. (2009).
105. Faegri, K. & Iversen, J. *Textbook of Pollen Analysis*. (John Wiley & Sons Ltd., Chichester, 1989).
106. McAndrews, J. H., McAndrews, J. H., Berti, A. A., Norris, G. & Museum, R. O. *Key to the Quaternary Pollen and Spores of the Great Lakes Region*. (Royal Ontario Museum, Toronto, 1973). https://doi.org/10.5962/bhl.title.60762.
107. Richard, P. J. H. Atlas pollinique des arbres et de quelques arbustes indigènes du Québec. *Nat. Can.* **97**, 24l–306l (1970).
108. Danesh, D. C., Gushulak, C. A. C., Moos, M. T., Karmakar, M. & Cumming, B. F. Changes in the prairie–forest ecotone in northwest Ontario (Canada) across the Holocene. *Quat. Res.* **106**, 44–55 (2022).
109. Juggins, S. rioja: Analysis of Quaternary Science Data. (2022).
110. Erb, M. P. et al. Reconstructing Holocene temperatures in time and space using paleoclimate data assimilation. *Clim. Past* **18**, 2599–2629 (2022).
111. He, F. & Clark, P. U. Freshwater forcing of the Atlantic Meridional Overturning Circulation revisited. *Nat. Clim. Chang.* **12**, 449–454 (2022).
112. Crema, E. R. & Bevan, A. Inference from large sets of radiocarbon dates: software and methods. *Radiocarbon* **63**, 23–39 (2021).
113. Gajewski, K. et al. The Canadian archaeological radiocarbon database (Card): Archaeological 14C dates in North America and their paleoenvironmental context. *Radiocarbon* **53**, 371–394 (2011).
114. Bird, D. et al. p3k14c, a synthetic global database of archaeological radiocarbon dates. *Sci. Data* **9**, 27 (2022).
115. Bluhm, L. E. & Surovell, T. A. Validation of a global model of taphonomic bias using geologic radiocarbon ages. *Quat. Res.* **91**, 325–328 (2019).
116. Polanco-Martinez, J. M., Medina-Elizalde, M. A., Goni, M. F. S. & Mudelsee, M. BINCOR: An R package for estimating the correlation between two unevenly spaced time series. *The R Journal* **11**, 170–184 (2019).
117. Gaboriau, D. M. et al. Temperature and fuel availability control fire size/severity in the boreal forest of central Northwest Territories. *Canada. Quat. Sci. Rev.* **250**, 106697 (2020).
118. Mudelsee, M. *Climate Time Series Analysis: Classical Statistical and Bootstrap Methods*. vol. 51 (Springer International Publishing, Cham, 2014).
119. Csárdi, G. et al. igraph for R: R interface of the igraph library for graph theory and network analysis. https://doi.org/10.5281/zenodo.8240644 (2023).
120. Wickham, H. ggplot2: Elegant Graphics for Data Analysis. (2006).
121. Spawn, S. A., Sullivan, C. C., Lark, T. J. & Gibbs, H. K. Harmonized global maps of above and belowground biomass carbon density in the year 2010. *Sci. Data* **7**, 112 (2020).
122. Walker, M. J. C. et al. Formal subdivision of the Holocene Series/Epoch: a Discussion Paper by a Working Group of INTIMATE (Integration of ice-core, marine and terrestrial records) and the Subcommission on Quaternary Stratigraphy (International Commission on Stratigraphy). *J. Quaternary Sci.* **27**, 649–659 (2012).

Acknowledgements

This research was facilitated by the financial and in-kind support extended by the Manitoba Hydro Forest Enhancement Program, Natural Sciences and Engineering Research Council of Canada (NSERC), The Canada Research Chair program, the University of Winnipeg, The Université du Québec en Abitibi-Témiscamingue, IRN Forêts Froides (CNRS, INEE), and the Canadian Forest Service. We express our gratitude to individuals including Benoit Brandelet, Laurent Bremond, Benoit Brossier, Cody Clovenchok, Karine Grotte, Johanna Hallmann, Kayla-Mae Hlushenko, Aurore Lucas, Raynald Julien, Brian Moons, Nia Perron, Johanna Robson, Zabrina Yaremko, France Conciatori, and Christine Simard for their contributions to field and laboratory work. We also thank Xiao Jing Guo for assistance with R. Acknowledgements are also extended to the personnel at Manitoba Conservation, Ontario Ministry of Natural Resources, and Manitoba Hydro for their guidance and assistance in this endeavor.

Author contributions

M.P.G., D.M.G., A.A.A., J.W., J.C.T. and Y.B. designed the study. A.A.A., J.W. and J.C.T. conducted fieldwork. M.P.G. analyzed data, created figures, and drafted the initial version of the manuscript. D.M.G. analyzed fire data and contributed to manuscript writing. K.G. and M.D.B. analyzed demographic data and contributed to manuscript writing. J.P. conducted pollen analysis and initial interpretation. All authors have made significant contributions to the final manuscript.

Competing interests

The authors declare that they have no known competing financial interests or personal relationships that could have appeared to influence the work reported in this paper.

Additional information

Supplementary information The online version contains supplementary material available at https://doi.org/10.1038/s43247-024-01340-8.

Correspondence and requests for materials should be addressed to Martin P. Girardin.

Peer review information *Communications Earth & Environment* thanks Anneli Poska and Philip Higuera for their contribution to the peer review of this work. A peer review file is available.